RSC Advances

PAPER

View Article Online
View Journal | View Issue

Cite this: *RSC Adv.*, 2022, **12**, 1718

Albumin grafted coaxial electrosparyed polycaprolactone-zinc oxide nanoparticle for sustained release and activity enhanced antibacterial drug delivery†

W. Pamoda Thavish D. Perera,[ab] D. M. Ranga K. Dissanayake,[*bc] Janitha M. Unagolla,[d] Rangika T. De Silva,[b] Sanjaya D. N. K. Bathige[b] and Lakshitha R. Pahalagedara[b]

One of the most serious issues faced by the healthcare sector is the development of multidrug resistance among various pathogens. It is such that developing new and more capable drugs takes far too long to counter such resistance. In order to overcome these concerns, this study focused on improving upon the coaxial electrospraying process by producing cloxacillin loaded albumin polycaprolactone (PCL) with a ZnO coating for sustained and activity enhanced drug delivery. Albumin-grafted, polycaprolactone-coated, zinc oxide-loaded cloxacillin (APCL-CLOX-ZnO) nanoparticles with a diameter of 85–110 nm were obtained *via* a coaxial electrospray technique. The encapsulation efficiency of cloxacillin of ZnO-CLOX was found to be approximately 60%. The loading efficiencies of ZnO-CLOX and APCL-CLOX-ZnO were found to be 40% and 28% respectively. Albumin was employed in order to impart immune evasion properties to the formulation. Drug-loaded ZnO NPs were analyzed using SEM, TEM, FT-IR and TGA. This novel formulation was shown to possess sustained release characteristics owing to the PCL and albumin coatings, relative to uncoated counterparts. ZnO-CLOX and APCL-CLOX-ZnO exhibited 72% and 52% cloxacillin release within 24 h. APCL-CLOX-ZnO exhibited potent antimicrobial activity against *S. epidermidis*, *B. cereus* and *P. aeruginosa* and some activity against *E. coli* with inhibition zones 32 ± 1.4, 34 ± 0.3, 32 ± 0.6 and 11 ± 0.4 mm, respectively. Cytotoxicity studies against murine preosteoblast cells revealed that the albumin-PCL coating served to drastically reduce initial toxicity against healthy mammalian cells. *In vitro* lung deposition study showed 70% of APCL-CLOX-ZnO particles can reach up to the alveoli level. Therefore, this novel coaxial nanoformulation may serve as a promising drug delivery platform for the treatment of bacterial infections including respiratory tract complications.

Received 24th October 2021
Accepted 3rd January 2022

DOI: 10.1039/d1ra07847j

rsc.li/rsc-advances

Introduction

The attraction of scientific and biomedical interest towards pulmonary drug delivery systems has mainly progressed in terms of local treatments for lung diseases where enhanced local targeting and reduced side effects with minute drug dosage administration were possible. Today, the paradigm has shifted towards inhaled antimicrobial therapy used with the high surface area and permeability of the lung.[1] There is, therefore, an escalating need to improve the efficacy of existing antibiotics against bacterial resistance *via* modulating drug delivery formulations.[2] Nanoparticles are considered to be the most promising tool for controlled and sustained release drug delivery systems.[3] Their advantage lies in their ability to carry the drug molecule to the site of action, improve bioavailability without side effects, and achieve safety and biocompatibility by delivering the drug to the intracellular level of different organs.[4] Moreover, physicochemical properties such as surface charge, size and hydrophobicity could be tweaked to elevate trans-mucosal absorption and nanoparticles have an inherent advantage over bulkier particles when it comes to cell penetration.[5,6] Consequently, nanoencapsulated drugs can sidestep many of the shortcomings of their non-encapsulated

[a]*Academy of the Sri Lanka Institute of Nanotechnology, Nanotechnology and Science Park, Mahenwatte, Pitipana, Homagama 10206, Sri Lanka*

[b]*Sri Lanka Institute of Nanotechnology, Nanotechnology and Science Park, Mahenwatte, Pitipana, Homagama 10206, Sri Lanka*

[c]*Department of Pharmacy and Pharmaceutical Sciences, University of Sri Jayewardenepura, Gangodawila, Nugegoda 10250, Sri Lanka. E-mail: rangad@sjp.ac.lk*

[d]*Department of Bioengineering, College of Engineering, University of Toledo, Toledo, OH 43607, USA*

† Electronic supplementary information (ESI) available. See DOI: 10.1039/d1ra07847j

counterparts, including the ability to evade bacterial resistance mechanisms.[2,7] Nanoparticles come in a variety of types such as liposomes, dendrimers, micelles, metallic and polymer-based.[8–10] Two processes are commonly used in the synthesis of drug-loaded nanoparticles, emulsification and electro-spraying.[2,11] Despite the ease of using the emulsification method it also offers several drawbacks that hinder effectiveness of its application, including varying particle sizes, poor encapsulation, and some serious issues such as the denaturing of the drugs loaded onto the nanoparticles.[12–14] These issues are largely addressed through the alternative, electrospraying method.[15]

Electrospraying allows the production of particles ranging from micro to nanoparticles while maintaining size uniformity.[11,16]

Studies in this regard have further concluded that quality of electrospray beads to be significantly higher, and the process itself to be more cost effective. Nonetheless, it must be noted that generic electrospray particles do not possess a protective covering, hence would give way to a burst release of the loaded drug upon application.[15,17] This drawback may be overcome through a more specialized technique referred to as coaxial electrospraying, which is capable of producing coated particles loaded with required drugs and other substances, without affecting their viability and morphology.[15,18]

Metal oxide nanoparticles can be functionalized using various chemical groups that permit them to bind to a variety of ligands, including antibodies and drugs.[9,19,20] Hence, an inorganic nanomaterial such as metal oxide is an attractive choice for the formulation of a robust drug-delivery platform. Zinc oxide is one such metal oxide that has shown potency as an antibacterial agent on its own against both Gram-positive and -negative bacteria.[10] This effect has been more pronounced at the nanoscale,[21] with these nanoparticles also having been found to be active against bacterial spores,[21] which are otherwise highly resistant.[22] ZnO nanoparticles (ZnO-NPs) can induce bacterial cell injury by generating hydrogen peroxide (H_2O_2), hydroxyl radicals (OH^-), and peroxide radicals (O_2^{2-}) at their surface, elevating membrane lipid peroxidation to ultimately cause membrane leakage of reducing sugars, DNA, proteins, and reduces cell viability of bacteria.[23,24]

It is evident from the literature that the antibacterial effect of ZnO-NPs depends on size, morphology and concentration.[25] Thus, the grafting of an antimicrobial drug agent onto its surface would enhance this inherent antimicrobial activity and produce a more effective antibacterial agent. Efforts have been made to synthesize porous ZnO nanoparticles that can adsorb drug moieties into their cavities. However, success has been limited to the *in vitro* level.[3] Drug-grafted ZnO nanoparticles can also be loaded into matrices made of micelles, polymers and liposomes.[14] Thus, drug-grafted ZnO particles are a possible counter to the emerging health crisis that is antibiotic resistance, whereby enhancing the activity of existing drugs against resistant bacterial strains without the need for *de novo* development of drugs. A sustained-release property would only add to the efficacy of such a platform. Coating with biodegradable proteins/polymers can facilitate both sustained circulatory persistence and slow release of the drug from the metal oxide's surface.[26]

Albumin is the most common endogenous protein carrier for a variety of xenobiotics, and is biodegradable, biocompatible, non-toxic and non-antigenic even when applied exogenously.[27] As a raw material, it is both readily available and affordable as well as safe to handle.[28] It is envisioned that albumin-coated ZnO nanoparticles would facilitate slow-release regimes and make the ZnO nanoparticle more biocompatible while avoiding the formation of both soft- and hard protein coronas, which ultimately lead to the rapid clearance of xenobiotics from circulation.[29]

Cloxacillin is a semisynthetic beta-lactamase-resistant penicillin-type antibiotic. It binds to and inactivates penicillin-binding proteins (PBPs) located on the inner membrane of the bacterial cell wall, preventing the cross-linkage of peptidoglycans, which are critical components of the bacterial cell wall. This leads to cell wall disruption and lysis.[30] The current adult dosage of cloxacillin for respiratory tract infections is 250–500 mg orally every 6 hours for 7–14 days, depending on the nature and severity of the infection, up to a maximum dosage is of 4 g per day.[31] Pneumonia has an indicated cloxacillin regimen of 500 mg orally every 6 hours for up to 21 days, depending on the nature and severity of the infection, again with a maximum daily dose of 4 g.[32] Therefore, it is very common to develop drug related toxicities as well as resistance with the respiratory system related drug regimes. However, reducing dose and direct delivery to the infected site can minimize above mentioned drawbacks. Therefore, the aim of this work was to synthesize albumin grafted (outer) and polycaprolactone (inner) coated zinc oxide-cloxacillin nanoparticles using a coaxial electrospray technique, for potential application as an aerosolized formulation of cloxacillin, which is non-existent at the time of writing, against respiratory tract infections: novel addition to the world's nanomedical arsenal.

Results and discussion

Morphological analysis

The scanning electron microscopy (SEM) images and transmission electron microscopy (TEM) image of zinc oxide nanoparticles, and APCL-ZnO-CLOX are pro-vided in Fig. 1. Both sets of particles were observed to be spherical in shape. ZnO nanoparticles were observed to possess an average diameter of approximately 85 ± 15 nm (within a range of 64–110 nm), while the coated, drug-loaded particles were of a 100 ± 18 nm average (within a range of 75–140 nm). SEM image of APCL-ZnO-CLOX is given in Fig. 1D. the particles are in different layers, therefore, focused particles are larger in size compare to the non-focus particles.

The prepared nanoparticles are highly stable in both aqueous and solid medium. The synthesis of nanoparticles was done at 600 °C hence provide high thermal stability. The thermal stability is also proven by the TGA analysis. Sedimentation of nanoparticles took place in aqueous medium and can be minimized by adding surfactant like CTAC or polysorbate.

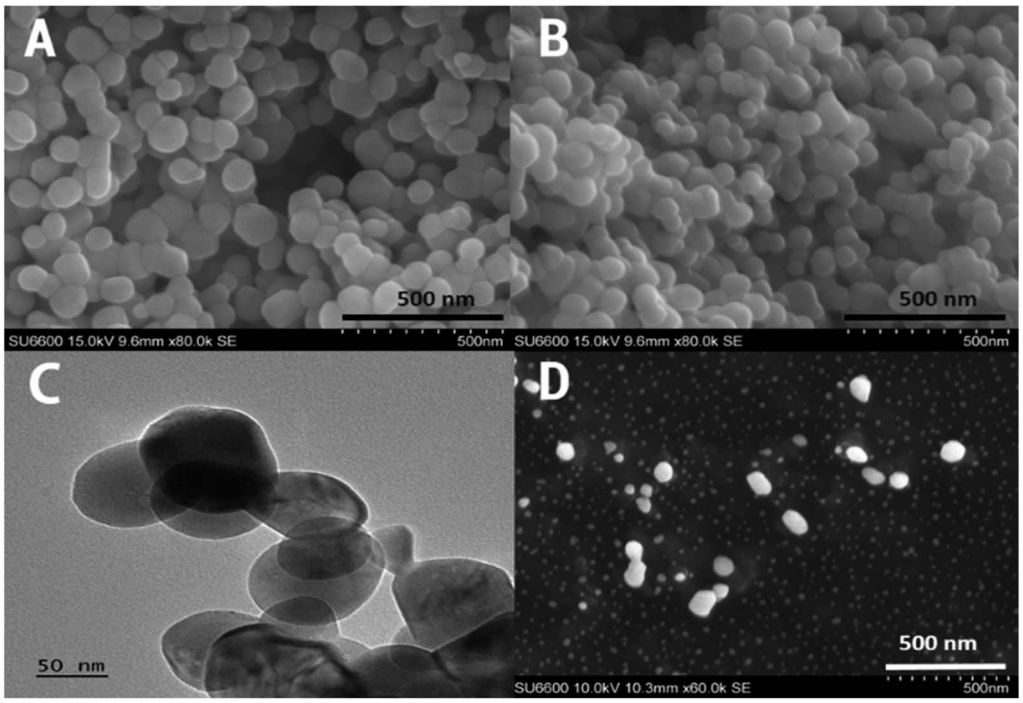

Fig. 1 Scanning electron microscope images of: (A and B) uncoated/bare ZnO nanoparticles, (C) transmission electron microscope image of ZnO nanoparticles, and (D) albumin-coated PCL-coated ZnO-cloxacillin nanoparticles (APCL-ZnO-CLOX).

Chemical characterization

The overlaid IR transmittance spectra of albumin (Fig. 2B) and ZnO-CLOX (Fig. 2D) both show a broad band above 3000 cm^{-1}, attributed to O–H stretching vibrations from adsorbed water molecules. The NH^{3+} and NH^{2+} symmetric bend observed at 1637 and 1533 cm^{-1} in the spectrum of the pure cloxacillin (Fig. 2A) appear to be masked by incorporation into the porous structure of the ZnO particles, disappearing into a broad, poorly-resolved set of peaks stretching from 1272–1703 cm^{-1}. Moreover, characteristic transmittance bands of the beta-lactam carbonyl (1770 cm^{-1}),[32] secondary amide carbonyl (1669 cm^{-1}),[33] aromatic ring (1619 cm^{-1}) and carboxylate carbonyl (1604 cm^{-1})[34] were observed in both the ZnO and ZnO-CLOX spectra. The PCL spectrum (Fig. 2E) displays the characteristic carbonyl band 1722 cm^{-1} and ether group at 1172 cm^{-1},[35] and these are also observed in the PCL-coated nanobead (Fig. 2C), confirming the presence of the polymer coating. The peak position of carbonyl group of PCL-ZnO-cloxacillin hybrid is shifted to 1722 cm^{-1}, which attributes strong interactions between PCL and cloxacillin molecules. The drug-loading process permitted cloxacillin to be grafted on the outer surface of ZnO NPs. The albumin spectrum (Fig. 2B) displays the characteristic amide I band 1645 cm^{-1} and amide II at 1535 cm^{-1},[36] but these are not visible in the coated samples' spectra possibly due to the irregular cluster of albumin moieties deposited on the PCL coating. In the spectrum of pure cloxacillin, the characteristic peak at 1650 cm^{-1} is due to amide linkages which supports well with the literature data. The appearance of drug peak at 1650 cm^{-1} in APCL-ZnO-CLOX nanocomposite confirms its presence in the hybrid. The peak position of carbonyl group of APCL-ZnO-CLOX nanocomposite is shifted to 1717 cm^{-1}, which attributes strong hydrogen bonded interactions between the carbonyl group of PCL and N–H and O–H groups of cloxacillin molecules. Similarly, C–O–C stretching peak of PCL at 1172 cm^{-1} is shifted to 1158 cm^{-1} in APCL–ZnO–CLOX nanocomposite. The hydroxyl groups which are available on the surface of ZnO NPs, are very likely to interact with N–H and O–H groups of cloxacillin *via* non-covalent interactions such as hydrogen bond and electrostatic interactions outer surface of ZnO NPs.[7]

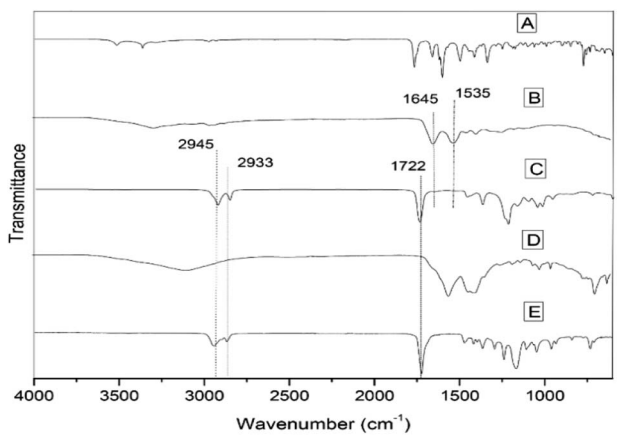

Fig. 2 FT-IR spectra of: (A) cloxacillin, (B) albumin, (C) APCL-ZnO-CLOX, (D) ZnO-CLOX and (E) PCL.

Physical characterization

Thermogravimetric analysis was carried out to assess any changes to the thermal stability of the raw materials when composited, and to estimate the amount of cloxacillin loaded onto the surface of the ZnO nanoparticle. The respective TGA graph is given in Fig. 3A. The initial weight loss (2%) of the bare nanoparticles at temperatures below 100 °C can be attributed to the elimination of surface-bound water. The mass loss due to the degradation of cloxacillin begins at 245 °C in both the pure- and ZnO-bound samples, with the C–O, C–C and COOH bonds breaking down by 250 °C as a result of the dehydration of saccharide chains. The weight loss of the ZnO-CLOX indicates that up to 55% of the coated particle consists of the drug alone.

The XRD pattern of ZnO nanoparticle is shown in Fig. 3B, with the results matching JCPDS card no. 00-0361451, showing the presence of crystalline ZnO in its customary wurtzite phase. The patterns exhibit characteristic 2θ/basal plane pairs of 31.78°/(100), 34.46°/(002), 36.29°/(101), 47.63°/(102), 56.70°/(110), 62.95°/(103), 68.04°/(200) and 69.07°/(201). No great differences are apparent in ZNP morphologies, but the lack of peaks other than those regarded as characteristic points to a high degree of sample purity.

Loading assessment and release study

The release of cloxacillin is caused mainly due the effect of passive diffusion. The encapsulation efficiency of cloxacillin on the ZnO nanoparticle was found to be approximately 60% (w/w) from both of the methods outlined in the experimental procedure (acid digestion and supernatant measurement). The loading efficiencies of cloxacillin of ZnO-CLOX and APCL-ZnO-CLOX were revealed 40% and 28% (w/w) respectively. The release profile of ZnO-CLOX shows an initial, rapid first phase up to 6 h, likely caused by the release of superficially-bound drug molecules. This is followed by a slower second phase up to 24 h, most likely a sign of the release of entrapped drug molecules within the pores of the ZnO nanoparticle.

The total drug content released by the ZnO-CLOX after 24 h stands at 74%, while that of the APCL-ZnO-CLOX stands at 52%.

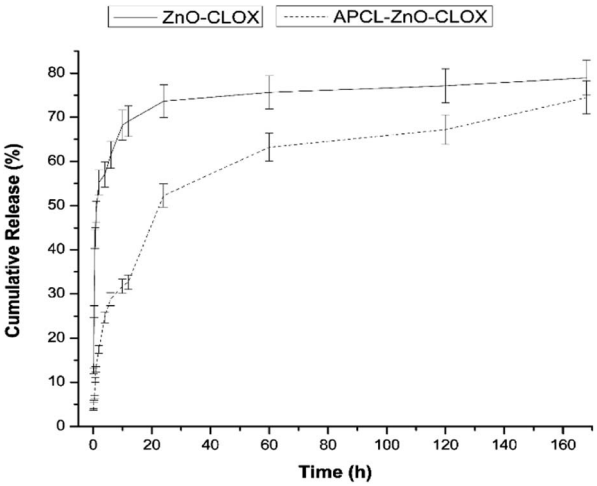

Fig. 4 Cumulative release of cloxacillin from cloxacillin-coated ZnO nanoparticles (ZnO-CLOX) and their albumin-coated PCL-coated counterparts (APCL-ZnO-CLOX) at pH 7.4. Results are presented as mean ± SD, $n = 3$.

At 168 h (7 days) these percentages increase to 79% and 74% respectively. After 24 h the uncoated formulation's release slows down to a large degree, almost plateauing, while the coated formulation undergoes a slowed (but still faster than the uncoated formulation) release (Fig. 4). Hence, this demonstrates that the PCL–albumin coating lends a considerable degree of sustained release character to the ZnO-CLOX system, extending the uncoated formulation's 24 h release to 168 h post-coating. There are several advantages in sustained-release formulations over traditional drug delivery system. *Via* the latter method, the drug is distributed body wide whereas sustained drug delivery allows release at the local site of infection and at a predetermined rate for a longer period of time. It leads to an increased therapeutic index and efficacy and reduces serum concentration and side effects to other organs. Localized drug delivery includes prolonged drug release, drug stability, and optimized drug absorption. As an important part, the drug

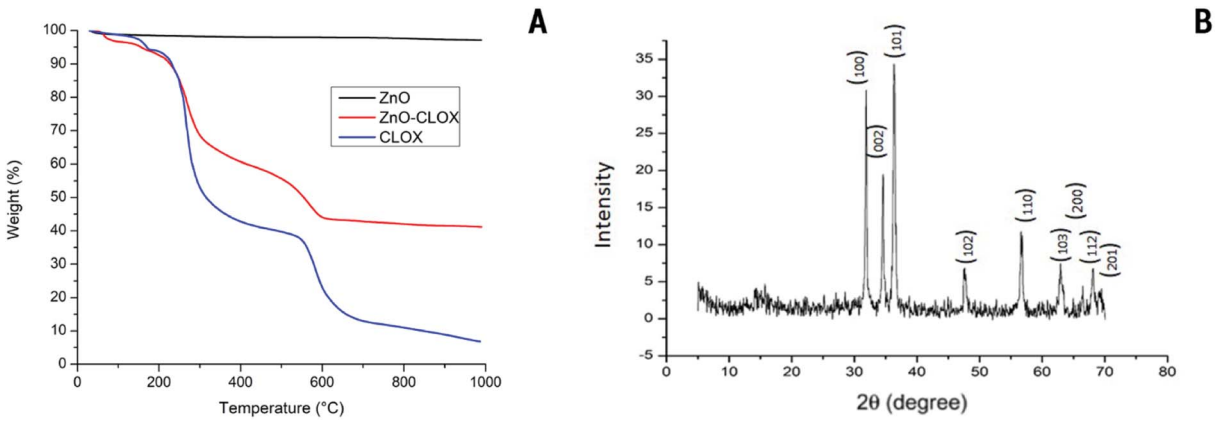

Fig. 3 (A) Overlaid thermograms of ZnO nanoparticles (ZnO), ZnO-cloxacillin nanobeads (ZnO-CLOX) and pure cloxacillin (CLOX). (B) XRD patterns obtained for the synthesized ZnO nanoparticles.

carrier acts in the drug delivery system and incorporates the drug, retains it, and release it progressively with time.

Antimicrobial study

The antibacterial activities of ZnO NPs, PCL-coated cloxacillin, ZnO-CLOX, APCL-ZnO-CLOX were tested by the disc-diffusion method on Gram-positive strains (*B. cereus* and *S. epidermidis*) as well as Gram-negative strains (*P. aeruginosa* and *E. coli*). CLOX showed the highest activity against all bacterial strains. The resulted inhibition zone on culture is shown in Fig. 5 and respective zone diameter is given in Table 1. This was to be expected, given the direct contact and free diffusion of the drug. Next highest inhibitions were shown by ZnO-CLOX followed by APCL-ZnO-CLOX. APCL-ZnO-CLOX inhibition capacity was slightly lower compare to ZnO-CLOX. Because, APCL-ZnO-CLOX contained less amount of cloxacillin compare to the equal weight of ZnO-CLOX due to coating materials. Further, the coating materials are extended the release of loaded drug material hence, reduce the diffusible drug amount. However, the inhibition differences were not significant and both nanomaterials contain potent antibacterial activity against both bacterial strains. The size of the inhibition zones among the samples tested appeared to vary dependent upon the type of bacteria and sample tested. *E. coli* appeared to be the least susceptible to the antibacterial activity of all nanocomposites tested, most likely due to the thicker cell membrane.

ZnO-CLOX showed higher inhibition compare to the pure cloxacillin. This indicated the synergetic activity of ZnO NPs and cloxacillin. Synergetic activities are more important in clinical setting in order to reduce the dose of particular antibiotic hence reduce the emergence of drug resistance and dose dependent toxicities. Therefore, this formulation automatically reduces the effective does of cloxacillin while increasing the antibacterial activity and more efficient to treat various bacterial infections.

Table 1 Results of the antibacterial assays of the various coated- and uncoated cloxacillin-loaded ZnO nanoparticles

	Inhibition diameter ±SD (mm)			
Material	*S. epidermidis*	*P. aeruginosa*	*B. cereus*	*E. coli*
ZnO	8 ± 1.3	13 ± 0.5	11 ± 1.4	10 ± 0.3
ZnO-CLOX	35 ± 1.5	37 ± 0.7	38 ± 1.2	12 ± 0.2
APCL-ZnO-CLOX	32 ± 1.4	34 ± 0.3	32 ± 0.6	11 ± 0.4
CLOX (+ve control)	40 ± 1.8	39 ± 0.6	43 ± 1.2	14 ± 0.5
Negative control	0	0	0	0

The antibacterial activity of nanoparticles is generally known to depend on size and shape, with size having an inversely proportional relationship with antimicrobial potential. Thus, nanoscale ZnO was expected to show better antibacterial activity than bulk ZnO.[37–39]

ZnO NPs are known to be toxic to host human cells, but only at very high concentrations. ZnO-based nanoparticles exert their antibacterial activity mainly by the production of reactive oxygen species (ROS) and zinc ions. Generated ROS (*i.e.* hydrogen peroxide (H_2O_2), OH^- (hydroxyl radicals), O_2^{2-} (peroxide radicals) and zinc ions) bind to the negatively-charged surface of the cell membrane, leading to disruption of cellular integrity and thus, cell death.[40–42]

Cloxacillin exerts its antibacterial activity *via* inactivating the penicillin-binding proteins (PBPs) located on the inner membrane of the bacterial cell wall, preventing the cross-linkage of peptidoglycans, which are critical components of the bacterial cell wall.[39] This leads to cell wall disruption and lysis. The low antibacterial activity observed against the Gram-negative bacteria is consistent with literature.[43,44] Gram-negative bacteria such as *E. coli* are known to be resistant to β-lactams such as cloxacillin due to endogenous production

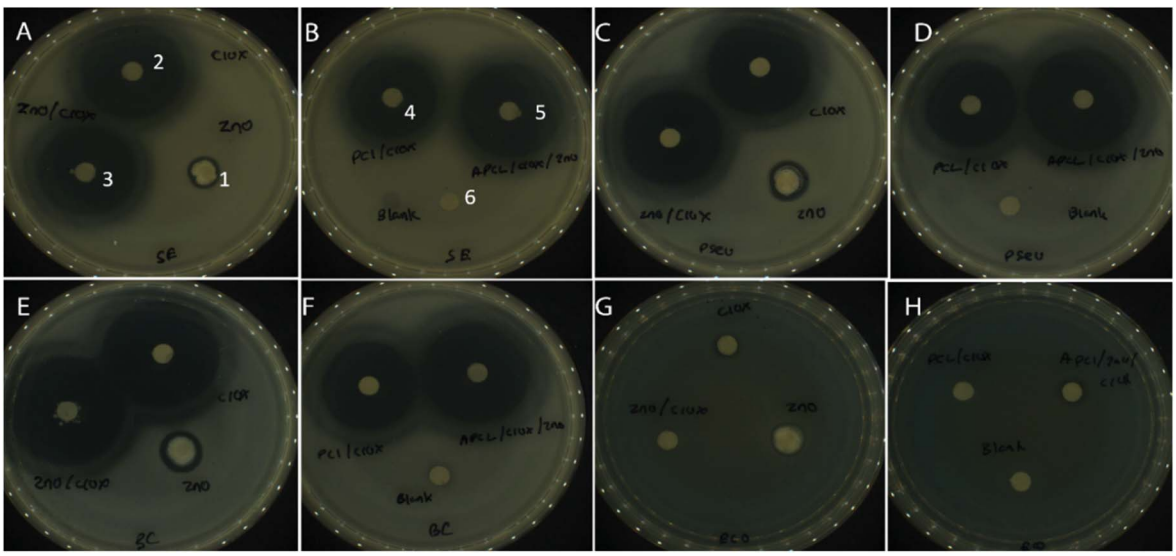

Fig. 5 Inhibition zones on cultures of: (A and B) *S. epidermidis*; (C and D) *P. aeruginosa*; (E and F) *Bacillus cereus*; (G and H) *E. coli*. Samples are labelled 1 (ZnO NPs), 2 (CLOX), 3 (ZnO-CLOX), 4 (PCL-coated CLOX), 5 (APCL-ZnO-CLOX) and 6 (negative control).

and secretion of β-lactamase/penicillinase, which largely nullifies the anti-PBP activity of the drug.[45,46]

Synergistic actions of semiconductor nanomaterials (ZnO, TiO_2 and SnO_2) with different antibiotics such as ampicillin, oxacillin, and norfloxacin against methicillin-resistant *S. aureus* have been previously reported.[47] Synergistic combination of ZnO with ciprofloxacin and gentamicin has also been effective in controlling *S. aureus*.[48,49] A recent study using zinc oxide nanoparticles and ZnO–gentamicin nanocomposites against *S. aureus*, *B. subtilis*, *E. coli*, and *P. aeruginosa* showed the nanocomposite to have higher efficacy than pristine zinc oxide nanoparticles or antibacterial agents on their own. From this, it is reasonable to conclude that there exists a synergetic effect between the ZnO and antimicrobial agents in the composites studied herein as well.

Cytotoxicity study

The bare ZnO nanoparticle and its cloxacillin-coated counterpart exhibit similar cytotoxicity profiles, decreasing cell viability to 50% and 45% respectively after 24 hours, and 17% and 15% respectively after 72 hours. PCL on its own has little effect on viability, exhibiting a 10–15% decrease in viability even after 72 hours. In the case of the albumin-coated formulation, a 45% increase in viability after 24 hours was observed: this can be attributed to albumin promoting cell proliferation, possibly by stimulating protein kinases.[50] After 48 hours, however, viability drops again (to approx. 60%) as the dissolution of the albumin coating leads to the ZnO and cloxacillin being exposed. Relative to this, ZnO-CLOX has a 3-fold higher 24 h toxicity and a 6.5-fold showed higher 72 h-toxicity (see Fig. 6A–F).

Fig. 6A–F shows the changes in cell growth and proliferation 24 hours after treatment with the various nanoformulations. The highest live cell count (relative to the negative control) was observed in the case of the APCL-ZnO-CLOX (Fig. 6F). Conversely, ZnO-CLOX (Fig. 6E) showed the lowest post-treatment cell viability. These observations and the general pattern observed in Fig. 6A–F corresponds with the WST-1 results presented in Fig. 6G (ESI Table S.1.† for full data set).

Despite the results of the FT-IR spectroscopy, the presence and advantage of the albumin coating becomes clear when comparing the results of the APCL-ZnO-CLOX with those of the PCL-ZnO-CLOX. Both the 24 h (70%) and 72 h (50%) viabilities of the latter are lower than those of the former. Taking the antibacterial assay as well, it is clear that the albumin coating helps the APCL-ZnO-CLOX formulation retain its sustained antibacterial activity while simultaneously reducing initial cytotoxic effects.

The toxicities of ZnO nanoparticles are well examined.[51] Basically, ZnO nanoparticles are nontoxic in lower concentrations. However, production of ROS in higher concentrations may cause some concentration dependent toxicities. There are number of products including topical creams, lotions, aqueous suspensions which contains ZnO nanoparticles.[52] This can be minimized by mixing or coating of ZnO Nps with nontoxic biocompatible PCL and albumin. The toxicity studies of this experiment proved the having such system.

In vitro lung deposition test

The results showed that 70% of the particles were collected to stage 2 chamber where only 15% collected to stage 1. This indicates the particles are small enough to carry drug to lower respiratory tract up to alveoli. There is a 15% difference between the total and collected value. This might be deposition of particles on the walls of apparatus and exhaled out by the pump. According to the literature, particles of size < 5 μm have the greatest possibility of deposition in the lung and particle with size < 2 μm can reach up to the alveoli.[53,54] However, the average size of the synthesized APCL-ZnO-CLOX is 0.1 μm which is 20 times smaller than particles which should have the diameter to reach alveoli. Hence, the synthesized final particle has more chance to accumulate inside the alveoli and above results confirm it. (Refer ESI Table S.2.† for complete data set).

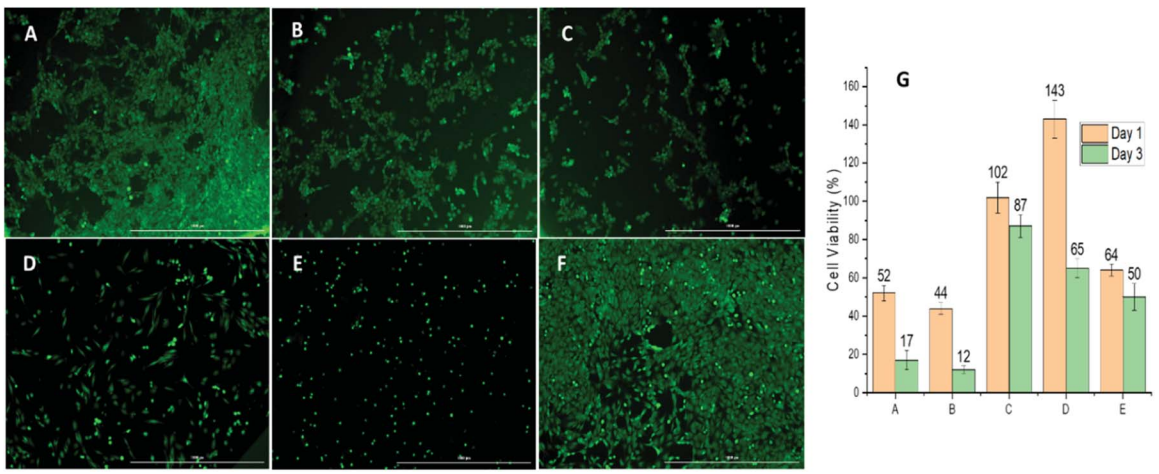

Fig. 6 (A–F) Changes in growth and proliferation induced by: (A) negative control, (B) PCL only, (C) PCL-coated ZnO, (D) ZnO NPs, (E) ZnO-CLOX, (F) APCL-ZnO-CLOX, after 24 hours. (G) Cytotoxicity of: (A) ZnO, (B) ZnO-CLOX, (C) PCL, (D) APCL-ZNO-CLOX and (E) PCL-Z.

The synthesized particles are classified as ultrafine particles according to the pulmonary drug delivery system where the size is <0.1 μm. Ultrafine particles of <100 nm size can largely deposit in the respiratory tract by random Brownian motion and these particles can reach the alveolar region. Particles in nanometer range are extensively taken up by macrophages, peritoneal macrophages and peripheral blood mononuclear cells. The uptake of these nanoparticles mainly takes place by pinocytosis and it is dependent on the concentration of particle in extracellular region and period of contact between macrophages and the particles. Therefore, estimation of particle size can give an idea of the drug deposition and penetration within the body.[53–55]

Experimental

Materials

Zinc nitrate, sodium hydroxide (99.8% purity) and cetrimonium chloride (CTAC) (25% solution) (all analytical grade) were purchased from Sigma (USA) and used without further purification. Bovine se-rum albumin was purchased from Sigma (USA). All aqueous solutions were prepared using distilled water, while distilled industrial-grade acetone and dimethyl sulfoxide (DMSO; SRLChem, India) were used as other solvents. The electrospray polymer polycaprolactone (MW = 10 000) was purchased from Sigma-Aldrich (USA) and the antimicrobial compound cloxacillin sodium was gifted by the State Pharmaceutical Manufacturing Corporation-Sri Lanka. Hydrochloric acid (37%) was purchased from SRLChem (India). Muller-Hinton agar (Hardy, USA) and phosphate buffered saline (PBS; Sigma GmbH, Germany) were used for microbiological studies. For culture of preosteoblasts, alpha-minimum essential media (α-MEM), fetal bovine serum (FBS), phosphate-buffered saline (PBS) and penicillin–streptomycin were purchased from Gibco Life Technologies (Thermo Fisher Scientific, USA). A water-soluble tetrazolium salts (WST-1) assay kit was obtained from Roche Diagnostics (USA).

Synthesis of zinc oxide nanoparticles

Aqueous solutions of zinc nitrate (0.5 M) and sodium hydroxide (1 M) were prepared, alongside a CTAC solution made with an adequate amount of the surfactant mixed with distilled water and stirred continuously at room temperature for 30 minutes until homogenous. This surfactant was then mixed well with the NaOH solution, following which the zinc nitrate was added dropwise into it while stirring at room temperature. The resulting white suspension was stirred in similar conditions for a further two hours. The precipitate was allowed to settle then filtered and rinsed with distilled water and methanol. The precipitate was then air-dried at room temperature and calcined at 600 °C in order to obtain the final product.

Drug loading

Cloxacillin was grafted onto the surface of the ZnO using an overnight stirring process and a standard vacuum evacuation process. Initially, 1 g of both zinc oxide and cloxacillin (1 : 1 mass ratio) were dispersed in 10 mL of distilled water and allowed to proceed through grafting under a stir speed of 500 rpm for 24 h at room temperature. The flask containing the resultant ZnO-cloxacillin (ZnO-CLOX) suspension was allowed to be evacuated using a vacuum pump for 30 minutes until the removal of entrapped air. After bubbling stopped, the suspension was kept under uninterrupted vacuum for 10 min to reach equilibrium. The entire vacuum evacuation cycle was repeated twice in order to facilitate the infiltration of cloxacillin into the surface of the ZnO nanoparticles. The suspension was then centrifuged and washed twice using distilled water to remove any unbound cloxacillin.

Synthesis of PCL-/albumin-coated ZnO-drug nanobeads

Coaxial electrospray in a vertical setup was used to prepare all coated nanoparticles: PCL-coated ZnO-CLOX (PCL-ZnO-CLOX) and albumin-coated PCL-ZnO-CLOX (APCL-ZnO-CLOX). The electrospray system consisted of a high voltage power supply, a coaxial needle (inner- and outer needle diameters of 0.5 mm and 0.6 mm respectively), two syringe pumps and a collector. The distance between positive (needle) and negative electrodes was maintained at 7 cm while the collector was 13 cm from the needle. PCL-ZnO-CLOX was synthesized by the use of a 1% ZnO-CLOX in a water/acetone (1 : 1 v/v) solvent system as the core solution, and a 0.25% (w/w) PCL solution in acetone was as the shell solution. The two solutions were sprayed with flow rates of 0.1 mL h^{-1} (core) and 0.3 mL h^{-1} (shell). APCL-ZnO-CLOX was synthesized by electrospraying a suspension of PCL-ZnO-CLOX into an albumin solution acting as a collector. An applied voltage of 4–5 kV was used throughout. PCL-coated cloxacillin was also synthesized using the above parameters for comparison.

Characterization of synthesized nanoparticles

Morphological analysis. The morphologies of nanoparticles synthesized using the methods set out above were evaluated using field-emission scanning electron microscopy (SEM; Hitachi SU6600 setup) and transmission electron microscopy (TEM; Jeol 2100 setup). All samples were subjected to gold sputtering prior to analysis.

Chemical characterization. Fourier-transform infrared (FT-IR) spectroscopic analysis was performed in order to confirm cloxacillin loading onto the surface of the ZnO nanoparticles, as well as to ascertain the presence of the various coatings applied. All spectra were obtained over the 4000–500 cm^{-1} region with 32 scans per measurement at a resolution of 4 cm^{-1} using a Bruker Vertex 80 Fourier transform infrared spectrophotometer (Bruker, USA). The spectrophotometer was equipped with a L-alanine doped triglycine sulfate (DLaTGS) detector and MIRacle single-reflection horizontal attenuated total reflectance (ATR) accessory (PIKE Technologies, USA) working at room temperature.

Physical characterization. The thermal stabilities of the synthesized nanoparticles were determined by thermogravimetric analysis (TGA; STD Q600 setup) over a temperature range of 25 to 1000 °C at a ramp of 20 °C min^{-1} in a nitrogen medium.

X-ray diffractometry was performed using a Bruker D8 Focus X-ray diffractometer with Cu-Kα radiation and an X-ray tube operating at 25 kV and 30 mA. Samples were scanned at a speed of 1° min^{-1} over a 2θ range of 5° to 70°.

Assessment of drug loading and encapsulation efficiencies. Loading and encapsulation efficiencies were measured through the use of two methods. Firstly, the supernatants derived from the washing steps of the initial loading procedure (set out previously) were collected, and diluted in 20% (v/v) dimethyl sulfoxide (DMSO). Aliquots from this were then subjected to UV spectrophotometry (Shimadzu UV-3600, Shimadzu Corporation, Japan), measuring the absorbance at 242 nm. This wavelength was found to be optimal, using solutions of pure cloxacillin in 20% aqueous DMSO. A standard curve of cloxacillin in 20% aqueous DMSO was made for the final quantification. Knowing the concentration of cloxacillin originally used for the loading procedure, the difference in the amount of cloxacillin before- and after the loading process could be calculated, and the amount of the drug loaded on the ZnO nanoparticles was established. Detail drug loading procedure is given in ESI.†

A second method involved the digestion of the ZnO-CLOX and APCL-ZnO-CLOX particles (25 mg) in a 0.1 M HCl solution while sonicating for 5 minutes. The resultant suspension was subjected to UV spectrophotometry and the pre-made standard curve used for quantification (Fig. S.1 in ESI†).

Assessment of drug release. Cumulative drug release from ZnO-CLOX and APCL-ZnO-CLOX were studied. Briefly, 100 mg of each was dispersed separately in 100 mL of phosphate-buffered saline (pH 7.4). Drug release was assessed over seven days at 37 °C, monitored *via* UV-spectrophotometry by measuring the absorbance of aliquots of the release buffer at 242 nm. The standard curve made for loading assessment was utilized herein as well.

Antibacterial study. The antibacterial activities of ZnO-CLOX, PCL-ZnO-CLOX, APCL-ZnO-CLOX and PCL-coated cloxacillin were tested against two Gram-positive bacteria (*Staphylococcus epidermidis* (ATCC 14990) and *Bacillus cereus* (ATCC 9027)) and two Gram-negative bacteria (*Pseudomonas aeruginosa* (ATCC 9027) and *Escherichia coli* (ATCC 35218)) using the disc diffusion method. Suspensions of the test microorganisms were prepared using a 24 h-old fresh culture, and the turbidity was compared with 0.5 McFarland standards. A 5 mL volume of each suspension was dispensed onto the surface of dried Mueller Hinton Agar (MHA) dishes and distributed throughout the surface. Non impregned antibiotic assay disc (6 mm) were loaded with 10 μL (100 mg mL^{-1}) of ZnO-CLOX, PCL-ZnO-CLOX, APCL-ZnO-CLOX, PCL-coated cloxacillin and were placed on the prepared MHA medium. A 10 μL of an aqueous cloxacillin solution (20 mg mL^{-1}) was used as the positive control and distilled water was used as the negative control. Overnight incubation at 37 °C followed, after which the different zones of inhibition were measured.[56,57]

Cytotoxicity study. Murine preosteoblast cell line (OB6) was cultured in α-MEM medium containing 15% FBS and 1% penicillin–streptomycin. The culture was maintained in a humidified incubator at 37 °C with 5% CO_2 and the culture medium was replaced every 3 days. After 80% confluency was reached, the cells were subcultured using 0.25% trypsin-EDTA solution. A cell density of 1×10^4 was to seed each well of a 24-well plate, with a seed volume of 300 μL per well, and incubated for 3 h to facilitate cell adhesion. Solutions of the ZnO-CLOX, APCL-ZnO-CLOX and PCL-coated cloxacillin were prepared in α-MEM growth media at concentrations of 20 mg mL^{-1}. Following the 3 h incubation, 700 μL of the nanomaterial solutions were placed in each well for a final concentration of 14 mg mL^{-1}. Blank wells that contained nanomaterials without cells and a negative control that contained cells without nanomaterials were also assessed.

Water-soluble tetrazolium salts (WST-1) assay was used to measure cell viability after nanomaterial application. The WST-1 assay was performed at day 1 and day 3. After each predetermined time point, the used α-MEM medium in a well was removed and wells were washed with PBS. Fresh α-MEM medium was added to each well with 10% (v/v) WST-1 reagent. The well plates were shaken for 2 min at 300 rpm for homogeneous mixing of WST-1 with the α-MEM medium. The plate was then incubated for 6 h at 37 °C and 5% CO_2. After 6 h, 100 μL from each well was transferred to 96-well plate and the level of dye formed was measured using a UV spectrophotometer (SpectraMax190, Molecular Devices) at a wavelength of 440 nm. All experiments were done in triplicate and mean cell viabilities were calculated against the negative control (cells only).[58]

***In vitro* lung deposition test.** Twin glass impinge set (Copley Scientific Limited, Nottingham, UK) was used to assess aerodynamic behavior of the final particle (APCL-ZnO-CLOX) which showed the highest biocompatibility. The experiment used clear HPMC capsule (size 3) contained 25 mg of dry powder testing material. The flow rate was adjusted to 60 L min^{-1} using critical flow controller. The capsule was loaded to monodose dry powder inhaler and the inhaler was attached to the impinger which containing 5 and 10 mL of 20% DMSO in stages 1 and 2, respectively to collect the aerosolized powder.[59] After inspiration, the glass impinger was detached, and each stage, the inhaler device, and emptied capsules were separately washed with appropriate volumes of 20% DMSO and placed into volumetric flasks. The collected samples were sonicated for 5 min and filtered. The cloxacillin concentrations of filtrates were determined using UV-vis spectrophotometer according the previously plotted calibration curve. The initial concentration of cloxacillin was determined by digesting 25 mg of APCL-ZnO-CLOX with 20% DMSO. The percentage values of particle distribution within each stage were calculated as a portion of the total cloxacillin amount.

Conclusions

Zinc oxide-cloxacillin incorporated nanoparticles coated with concentric layers of polycaprolactone and albumin were fabricated successfully *via* coaxial electrospraying technique. These ranged in size from 85 to 100 nm. The loading efficiency of cloxacillin onto bare ZnO nanoparticles was confirmed using thermogravimetry and a UV-vis based drug release study, which revealed the encapsulation to be between 55% and 60 wt%. The albumin/PCL coating was shown to extend the cloxacillin's

release (74%) from the ZnO particles from 24 to 168 hours, imparting a sustained release character to the formulation. With the release maintained at a predetermined rate for a longer time, the release profile expects to benefit and in sustained drug delivery, the drug released at the local site of infection but in the traditional drug delivery the drug distributes all over the body. This leads to increased therapeutic index and therapeutic efficacy. This reduces serum concentration and side effects on other organs. Drug stability, optimized drug absorption and prolonged drug release can be achieved by localized drug delivery. The antimicrobial studies showed the albumin/PCL-coated formulation to be effective against mostly Gram-positive strains while presenting some activity against Gram-negative strains. This is likely due to the choice of antibiotic used. The cytotoxicity/cell viability studies revealed that the synthesized nanoparticles are non-toxic to cells and human body, with the albumin acting to protect cells from cytotoxic effects up to at least 24 hours post-encounter. *In vitro* lung deposition study showed the large portion of albumin/PCL-coated particles can reach up to alveoli level hence suitable for lower respiratory infections. This formulation thus holds great potential as a drug delivery platform for the treatment of respiratory tract complications, possibly paving the way for a biocompatible cloxacillin-based inhaler in future.

Author contributions

DMRK Dissanayake: conceptualization, supervision, investigation, writing – reviewing and editing. WPTD Perera: data curation, writing – original draft preparation, investigation. RT de Silva, LR Pahalagedara, SDNK Bathige: methodology, writing – reviewing and editing. JM Unagolla: investigation, methodology.

Conflicts of interest

There are no conflicts to declare.

Acknowledgements

This study was supported by the Research Fund of the Sri Lanka Institute of Nanotechnology (PRO0088) & University research grant ASP/01/RE/AHS/2021/90. The authors would like to thank Dr Malini Damayanthi and Dr Induni Siriwardana for their support in SEM imaging, and Kalindu Perera for assistance with artwork and editing.

Notes and references

1 R. Singh and J. W. Lillard, *Exp. Mol. Pathol.*, 2009, **86**, 215–223.
2 S. Onoue, S. Yamada and H. Chan, *Int. J. Nanomed.*, 2014, 1025–1037.
3 J. K. Patra, G. Das, L. F. Fraceto, E. V. R. Campos, M. D. P. Rodriguez-Torres, L. S. Acosta-Torres, L. A. Diaz-Torres, R. Grillo, M. K. Swamy, S. Sharma, S. Habtemariam and H.-S. Shin, *J. Nanobiotechnol.*, 2018, **16**, 71.
4 S. Senapati, A. K. Mahanta, S. Kumar and P. Maiti, *Signal Transduction Targeted Ther.*, 2018, **3**, 7.
5 S. Cao, S. Xu, H. Wang, Y. Ling, J. Dong, R. Xia and X. Sun, *AAPS PharmSciTech*, 2019, **20**, 190.
6 T. M. M. Ways, K. W. Ng, W. M. Lau and V. V. Khutoryanskiy, *Pharmaceutics*, 2020, **12**, 1–25.
7 L. Wang, C. Hu and L. Shao, *Int. J. Nanomed.*, 2017, **12**, 1227–1249.
8 X. Yang, J. J. Grailer, I. J. Rowland, A. Javadi, S. A. Hurley, D. A. Steeber and S. Gong, *Biomaterials*, 2010, **31**, 9065–9073.
9 R. T. De Silva, R. K. Dissanayake, M. M. M. G. P. G. Mantilaka, W. P. S. L. Wijesinghe, S. S. Kaleel, T. N. Premachandra, L. Weerasinghe, G. A. J. Amaratunga and K. M. N. de Silva, *ACS Appl. Mater. Interfaces*, 2018, **10**, 33913–33922.
10 V. Lakshmi Prasanna and R. Vijayaraghavan, *Langmuir*, 2015, **31**, 9155–9162.
11 J. Chen, Y. Cui, X. Xu and L. Q. Wang, *Colloids Surf., A*, 2018, **547**, 1–7.
12 H. G. Lee, D. W. Kim and C. W. Park, *J. Pharm. Invest.*, 2018, **48**, 603–616.
13 K. H. Bae, H. J. Chung and T. G. Park, *Mol. Cells*, 2011, **31**, 295–302.
14 A. P. Singh, A. Biswas, A. Shukla and P. Maiti, *Signal Transduction Targeted Ther.*, 2019, **4**, 1–21.
15 R. K. Dissanayake, K. D. C. Perera, W. P. T. D. Perera, W. P. S. L. Wijesinghe and J. M. Unagolla, *J. Nanomater.*, 2021, **2021**, 1–9.
16 R. S. Andre, L. A. Mercante, H. d. M. Brandão, R. Schneider, D. S. Correa and L. H. C. Mattoso, *React. Funct. Polym.*, 2018, **132**, 26–35.
17 B. T. Midhun, K. T. Shalumon, K. Manzoor, R. Jayakumar, S. V. Nair and M. Deepthy, *J. Biomater. Sci., Polym. Ed.*, 2011, **22**, 2431–2444.
18 R. T. De Silva, R. K. Dissanayake, M. M. M. G. P. G. Mantilaka, W. P. S. L. Wijesinghe, S. S. Kaleel, T. N. Premachandra, L. Weerasinghe, G. A. J. Amaratunga and K. M. N. De Silva, *ACS Appl. Mater. Interfaces*, 2018, **10**, 33913–33922.
19 R. T. De Silva, M. M. M. G. P. G. Mantilaka, K. L. Goh, S. P. Ratnayake, G. A. J. Amaratunga and K. M. N. de Silva, *Int. J. Biomater.*, 2017, **2017**, 1–9.
20 W. P. T. D. Perera, R. K. Dissanayake, U. I. Ranatunga, N. M. Hettiarachchi, K. D. C. Perera, J. M. Unagolla, R. T. De Silva and L. R. Pahalagedara, *RSC Adv.*, 2020, **10**, 30785–30795.
21 K. S. Siddiqi, A. ur Rahman, Tajuddin and A. Husen, *Nanoscale Res. Lett.*, 2018, **13**, 141.
22 H. Li, Q. Chen, J. Zhao and K. Urmila, *Sci. Rep.*, 2015, **5**, 1–13.
23 H. Zhang, B. Chen, H. Jiang, C. Wang, H. Wang and X. Wang, *Biomaterials*, 2011, **32**, 1906–1914.
24 S. Ostrovsky, G. Kazimirsky, A. Gedanken and C. Brodie, *Nano Res.*, 2009, **2**, 882–890.
25 K. R. Raghupathi, R. T. Koodali and A. C. Manna, *Langmuir*, 2011, **27**, 4020–4028.

26 M. J. Limo, A. Sola-Rabada, E. Boix, V. Thota, Z. C. Westcott, V. Puddu and C. C. Perry, *Chem. Rev.*, 2018, **118**, 11118–11193.
27 A. Saha, N. Pradhan, S. Chatterjee, R. K. Singh, V. Trivedi, A. Bhattacharyya and D. Manna, *ACS Appl. Nano Mater.*, 2019, **2**, 3671–3683.
28 M. Kopp, S. Kollenda and M. Epple, *Acc. Chem. Res.*, 2017, **50**, 1383–1390.
29 K. R. Upadhya, L. Shenoy and R. Venkateswaran, *J. Anaesthesiol., Clin. Pharmacol.*, 2018, **34**, 46–50.
30 C. Wintenberger, B. Guery, E. Bonnet, B. Castan, R. Cohen, S. Diamantis, P. Lesprit, L. Maulin, Y. Péan, E. Peju, L. Piroth, J. P. Stahl, C. Strady, E. Varon, F. Vuotto and R. Gauzit, *Médecine et Maladies Infectieuses*, 2017, **47**, 92–141.
31 Y. K. Yoon, C. S. Park, J. W. Kim, K. Hwang, S. Y. Lee, T. H. Kim, D. Y. Park, H. J. Kim, D. Y. Kim, H. J. Lee, H. Y. Shin, Y. K. You, D. A. Park and S. W. Kim, *Infect. Chemother.*, 2017, **49**, 326–352.
32 H. C. Neu, *Appl. Microbiol.*, 1969, **17**, 783–786.
33 G. Nicola, J. Tomberg, R. F. Pratt, R. A. Nicholas and C. Davies, *Biochemistry*, 2010, **49**, 8094–8104.
34 B. C. Smith, *Spectroscopy*, 2017, **32**(9), 31–36.
35 K. Gipson, K. Stevens, P. Brown and J. Ballato, *J. Spectrosc.*, 2015, **2015**, 1–9.
36 D. Usoltsev, V. Sitnikova, A. Kajava and M. Uspenskaya, *Biomolecules*, 2019, **9**, 359.
37 Z. Emami-Karvani, *Afr. J. Microbiol. Res.*, 2012, **5**, 1368–1373.
38 P. J. P. Espitia, N. d. F. F. Soares, J. S. d. R. Coimbra, N. J. de Andrade, R. S. Cruz and E. A. A. Medeiros, *Food Bioprocess Technol.*, 2012, **5**, 1447–1464.
39 I. Nikolaidis, S. Favini-Stabile and A. Dessen, *Protein Sci.*, 2014, **23**, 243–259.
40 M. Kundu, P. Sadhukhan, N. Ghosh, S. Chatterjee, P. Manna, J. Das and P. C. Sil, *J. Adv. Res.*, 2019, **18**, 161–172.
41 X. Cai, Y. Luo, W. Zhang, D. Du and Y. Lin, *ACS Appl. Mater. Interfaces*, 2016, **8**, 22442–22450.
42 P. P. Patil, J. V. Meshram, R. A. Bohara, S. G. Nanaware and S. H. Pawar, *New J. Chem.*, 2018, **42**, 14620–14629.
43 M. Laws, A. Shaaban and K. M. Rahman, *FEMS Microbiol. Rev.*, 2019, **43**, 490–516.
44 G. M. S. Soares, L. C. Figueiredo, M. Faveri, S. C. Cortelli, P. M. Duarte and M. Feres, *J. Appl. Oral Sci.*, 2012, **20**, 295–309.
45 A. Asli, E. Brouillette, K. M. Krause, W. W. Nichols and F. Malouin, *Antimicrob. Agents Chemother.*, 2016, **60**, 752–756.
46 P. Bajaj, N. S. Singh and J. S. Virdi, *Front. Microbiol.*, 2016, **7**, 417.
47 S.-H. Mun, D.-K. Joung, Y.-S. Kim, O.-H. Kang, S.-B. Kim, Y.-S. Seo, Y.-C. Kim, D.-S. Lee, D.-W. Shin, K.-T. Kweon and D.-Y. Kwon, *Phytomedicine*, 2013, **20**, 714–718.
48 P. Patra, S. Mitra, N. Debnath, P. Pramanik and A. Goswami, *Bull. Mater. Sci.*, 2014, **37**, 199–206.
49 G. Voicu, O. Oprea, B. S. Vasile and E. Andronescu, *Digest Journal of Nanomaterials and Biostructures*, 2013, **8**, 1191–1203.
50 L. Gallego, L. Junquera, Á. Meana, M. Álvarez-Viejo and M. Fresno, *J. Biomater. Appl.*, 2010, **25**, 367–381.
51 L. Vimercati, D. Cavone, A. Caputi, L. De Maria, M. Tria, E. Prato and G. M. Ferri, *Front. Public Health*, 2020, **8**, 1–19.
52 S. Anjum, M. Hashim, S. A. Malik, M. Khan, J. M. Lorenzo, B. H. Abbasi and C. Hano, *Cancers*, 2021, **13**, 4570.
53 A. Yıldız-Peköz and C. Ehrhardt, *Pharmaceutics*, 2020, **12**, 1–7.
54 S. P. Newman, *Ther. Delivery*, 2017, **8**, 647–661.
55 L. Ely, W. Roa, W. H. Finlay and R. Löbenberg, *Eur. J. Pharm. Biopharm.*, 2007, **65**, 346–353.
56 A. Kirisanth, M. N. M. Nafas, R. K. Dissanayake and J. Wijayabandara, *Evid. base Compl. Alternative Med.*, 2020, 3479851.
57 W. D. Ratnasooriya, S. G. Ratnasooriya and R. Dissanayake, *J. Coastal Life Med.*, 2016, **4**, 623–627.
58 B. Gaihre, J. M. Unagolla, J. Liu, N. A. Ebraheim and A. C. Jayasuriya, *ACS Biomater. Sci. Eng.*, 2019, **5**, 4587–4600.
59 H. Omer, N. Husein and H. Hamadameen, *Zanco Journal of Medical Sciences*, 2019, **23**, 74–80.